Human Molecular Genetics, 2014, Vol. 23, No. 11 **2901–2913**
doi:10.1093/hmg/ddu003
Advance Access published on January 8, 2014

Human COX20 cooperates with SCO1 and SCO2 to mature COX2 and promote the assembly of cytochrome *c* oxidase

Myriam Bourens[1], Aren Boulet[3], Scot C. Leary[3] and Antoni Barrientos[1,2,*]

[1]Department of Neurology, and [2]Department of Biochemistry and Molecular Biology, University of Miami Miller School of Medicine, Miami, FL, USA and [3]Department of Biochemistry, University of Saskatchewan, Saskatoon, Canada

Received November 8, 2013; Revised December 10, 2013; Accepted January 2, 2014

Cytochrome *c* oxidase (CIV) deficiency is one of the most common respiratory chain defects in patients presenting with mitochondrial encephalocardiomyopathies. CIV biogenesis is complicated by the dual genetic origin of its structural subunits, and assembly of a functional holoenzyme complex requires a large number of nucleus-encoded assembly factors. In general, the functions of these assembly factors remain poorly understood, and mechanistic investigations of human CIV biogenesis have been limited by the availability of model cell lines. Here, we have used small interference RNA and transcription activator-like effector nucleases (TALENs) technology to create knockdown and knockout human cell lines, respectively, to study the function of the CIV assembly factor COX20 (FAM36A). These cell lines exhibit a severe, isolated CIV deficiency due to instability of COX2, a mitochondrion-encoded CIV subunit. Mitochondria lacking COX20 accumulate CIV subassemblies containing COX1 and COX4, similar to those detected in fibroblasts from patients carrying mutations in the COX2 copper chaperones SCO1 and SCO2. These results imply that in the absence of COX20, COX2 is inefficiently incorporated into early CIV subassemblies. Immunoprecipitation assays using a stable *COX20* knockout cell line expressing functional COX20-FLAG allowed us to identify an interaction between COX20 and newly synthesized COX2. Additionally, we show that SCO1 and SCO2 act on COX20-bound COX2. We propose that COX20 acts as a chaperone in the early steps of COX2 maturation, stabilizing the newly synthesized protein and presenting COX2 to its metallochaperone module, which in turn facilitates the incorporation of mature COX2 into the CIV assembly line.

INTRODUCTION

Defects in the assembly and function of cytochrome *c* oxidase or mitochondrial respiratory chain complex IV (CIV) are a frequent cause of oxidative phosphorylation disorders in humans. Patients suffering from CIV-related mitochondrial diseases present with heterogeneous clinical phenotypes ranging from encephalomyopathy, hypertrophic cardiomyopathy and liver disease to Leigh's syndrome (1–4). Over the last 30 years, progress made on the characterization of CIV structure, biogenesis and function (5–11) has yielded considerable insight into the molecular basis of many of these human disorders.

CIV is an electron-driven proton pump that catalyzes the reduction of dioxygen to water (12). As the terminal oxidase of the mitochondrial respiratory chain, it participates in the formation of an electrochemical proton gradient that is subsequently used by the mitochondrial F_1F_o ATPase to drive ATP synthesis (13). Human CIV is formed by 13 subunits of dual genetic origin. The mitochondrial genome encodes the three core, catalytic subunits (COX1, 2 and 3), whereas the nuclear genome encodes the remaining subunits. COX1 and COX2 coordinate metal prosthetic groups essential for electron transfer. COX1 coordinates one redox center with a heme *a* and a second binuclear center containing a heme a_3 paired with a Cu(I) atom (Cu_B site). The third redox center of the enzyme resides in COX2 and is formed by two copper ions of mixed valences (Cu_A site). During catalysis, electrons are transferred from ferrocytochrome *c* to the Cu_A active site and subsequently to the heme *a* site. From heme *a*, electrons are transferred to the heme a_3-Cu_B binuclear center where bound molecular oxygen is ultimately reduced to water.

CIV biogenesis has been described as a linear process with the different subunits being added in an ordered manner (14).

*To whom correspondence should be addressed at: Departments of Neurology and Biochemistry and Molecular Biology, University of Miami Miller School of Medicine, RMSB 2067, 1600 NW 10th Ave., Miami, FL 33136, USA. Tel: +1 3052438683; Fax: +1 3052437404; Email: abarrientos@med.miami.edu

Additionally, data obtained in *Saccharomyces cerevisiae* indicate that at least the catalytic subunits COX1 and COX2 form associations with assembly factors in individual assembly lines prior to their incorporation into the general CIV assembly line (15,16). CIV assembly is initiated around a seed formed by COX1, and proceeds with the formation of subassemblies of progressively increasing complexity (14). Maturation of COX1 seems to be the first step in the process, with the insertion of its metal co-factors only occurring once COX1 has been inserted into the membrane (17). COX4 and COX5a are then added to mature COX1 to form the S2 intermediate. Incorporation of COX2 and most of the remaining structural subunits results in the formation of the S3 intermediate. Finally, insertion of COX6a and COX7a/b produces the CIV monomer (14).

Progression through all stages of the CIV assembly process requires a large number of nucleus-encoded proteins termed COX assembly factors, many of which were first identified in *S. cerevisiae* (18,19). For example, yeast Cox20 is involved in Cox2 biogenesis by acting as a Cox2-specific chaperone. Both Cox20 and Cox2 have two transmembrane domains, with their N- and C-termini protruding into the intermembrane space. Cox20 binds to newly synthesized Cox2, which in yeast is synthesized as a precursor protein, and presents it to the inner membrane peptidase (IMP) complex to facilitate the cleavage of its N-terminal leader sequence (16,20). Cox20 also fulfills an essential role in the translocation of the C-terminus of Cox2 through the membrane. The metallochaperone Sco1 then interacts with Cox2 to facilitate the maturation of its Cu_A site (21). Over the last 15 years, *in silico* approaches and the analysis of tissues and cultured cell lines derived from patients suffering from CIV deficiencies have allowed for the identification and characterization of both evolutionarily conserved and mammalian-specific COX assembly factors (22–26). Human SCO1 and SCO2 are homologues of yeast Sco1 and are both required for COX2 metallation (27), with mutations in either *SCO* gene causing mitochondrial encephalocardiomyopathies or hepatopathies (28,29). Recently, a mitochondrial disorder associated with CIV deficiency was reported in two families carrying the same homozygous mutation in *FAM36A* (23,30) the open reading frame encoding the human homologue of yeast Cox20 (31). Human COX20 was found to be important for the assembly of CIV, probably by acting on COX2 (23), but its specific role in holoenzyme biogenesis has yet to be fully described. We therefore sought to further elucidate how human COX20 stabilizes COX2, to allow for its efficient maturation and insertion into assembling CIV. By using siRNA and transcription activator-like effector nucleases (TALENs) technology (32–34) to silence *COX20* expression in human cell lines, we demonstrated that human COX20 plays a role as a COX2 chaperone in the early steps of COX2 biogenesis. We also showed that a transient complex composed of newly synthesized COX2, COX20, and the copper chaperones SCO1 and SCO2 is formed and that it facilitates COX2 membrane insertion, maturation and ultimately assembly of the holoenzyme.

RESULTS

RNA_i silencing of human *COX20* causes an isolated CIV deficiency by destabilizing newly synthesized COX2

To analyze the role of COX20 in mitochondrial metabolism, we started by conducting siRNA-specific knockdown of endogenous *COX20* expression in cultured HEK293T cells. Compared with the mock control, transient transfection of two different *COX20*-specific siRNA duplexes (Fig. 1A) led to an ~80% reduction in *COX20* mRNA levels at Days 1, 2 and 3 (Fig. 1B and C). Immunoblot analysis confirmed the efficacy of knockdown at the protein level. Even though our affinity-purified anti-COX20 antibody cross-reacts strongly and non-specifically with larger proteins, it clearly detects a protein that migrates at the predicted molecular weight of COX20 (15 kDa) whose steady-state levels are markedly attenuated in *COX20*-silenced cells (Fig. 1D). The net effect of *COX20* silencing on mitochondrial metabolism was a decrease in endogenous cell respiratory capacity (Fig. 1E). The abundance of COX2 and COX3 subunits was significantly decreased in *COX20*-silenced cells, whereas the levels of COX1 or of subunits of other oxidative phosphorylation complexes were not affected (Fig. 1F). Consistent with these observations, Blue Native-polyacrylamide gel electrophoresis (BN-PAGE) analyses showed that *COX20* silencing produced an isolated CIV deficiency (Fig. 1G) and led to the accumulation of assembly intermediates containing COX1 alone (S1) or at least COX1 and COX4 (S2 and S3) (Fig. 1H). These subassemblies correspond to the intermediates observed in cell lines derived from patients with mutations in the COX2 metallochaperone SCO1 or in the CIV assembly factor SURF1 (Fig. 1I). The CIV assembly defect in *COX20*-silenced cells is not due to a gross defect in COX2 synthesis as assessed by *in vivo* pulse-labeling of mitochondrial translation products. Rather, chase-labeling experiments showed that when COX20 levels are limiting, newly synthesized COX2 is unstable and most of it is rapidly degraded within 2 h of the chase (Fig. 1J). ATP6 was also found to be labile in this chase assay, although we did not observe any effect on the steady-state levels of the F_1F_o ATPase (Fig. 1G). These results are consistent with the recently reported phenotype in fibroblasts derived from a *COX20* patient (23), and suggest that COX2 is less stable upon depletion of COX20 because of a defect in its membrane insertion, maturation of its Cu_A site and/or a block in its incorporation into the S2 assembly intermediate.

Generation of a human *COX20* knockout cell line using TALENs in HEK293T cells

Working with RNA_i-silenced cells has its practical limitations because one cannot exclude the possibility of residual *COX20* expression, and because it is difficult to obtain the number of cells that are required to isolate enough mitochondria for extensive biochemical analyses. Therefore, to further understand the exact function of COX20 in CIV biogenesis, we turned to a gene-editing approach and used transcription activator-like effector nucleases (TALENs) technology to create a stable human *COX20* knockout line in HEK293T cells. TALENs are sequence-specific nucleases created by the fusion of the catalytic domain of an endonuclease (the *Fok*I restriction enzyme) to TALE proteins, a large group of bacterial plant pathogen proteins that have emerged as alternatives to zinc finger proteins because of their very high fidelity DNA-binding capacity (32,34). We used the services of Cellectis Bioresearch (Paris, France) to design and generate the 'best hit' TALEN binding pair to disrupt *COX20* expression in HEK293T cells, which target a region within the first exon of the gene that is directly downstream of the translation start codon (Fig. 2A). Although

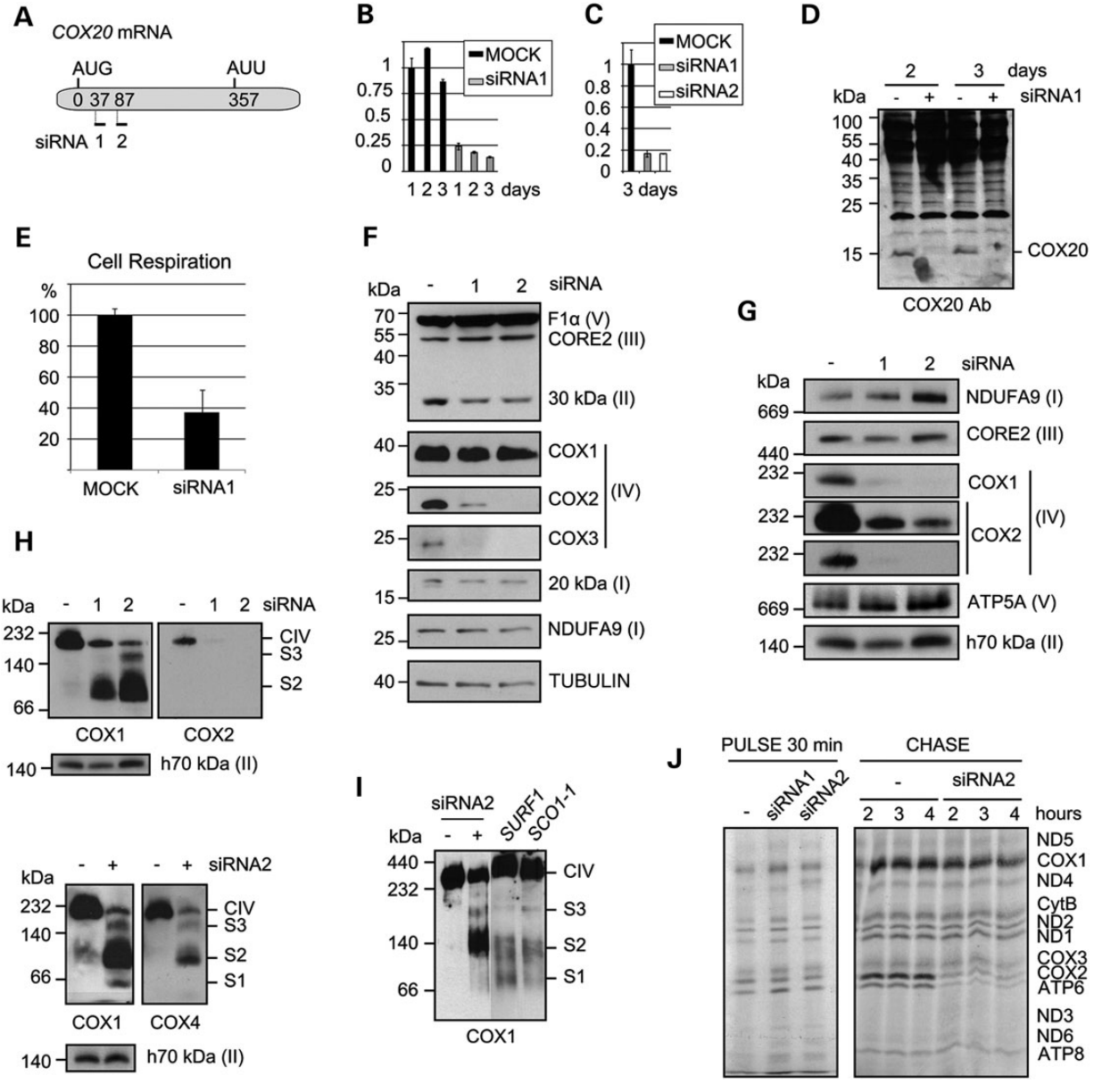

Figure 1. COX20 knockdown causes an isolated CIV deficiency by destabilizing newly synthesized COX2. (**A**) Schematic representation of the *COX20* mRNA regions that are recognized by siRNA duplex oligonucleotides #1 and #2. (**B**) and (**C**) *COX20* mRNA abundance in HEK293T cells transfected with 10 nM of the indicated *COX20* siRNA duplex, estimated by qPCR. *COX20* mRNA levels were normalized to those of HPRT1 (hypoxanthine phosphoribosyltransferase 1) and expressed as a percentage of the abundance at Day 1. (**D**) Immunoblot analysis of COX20 protein levels in extracts from mock-transfected cells and cells transfected with 10 nM of siRNA #1. (**E**) Endogenous cell respiration following silencing of *COX20* expression for 10 days with 10 nM of siRNA #1. Data are expressed as percentage of the respiratory rate of mock-transfected cells. (**F**) Steady-state levels of representative subunits of the oxidative phosphorylation complexes (indicated in parentheses) in whole cells extracts from mock-treated HEK293T cells (−) and cells transfected with 10 nM of siRNA #1 or #2 for 6 days. Tubulin was used as a loading control. (**G**) and (**H**) BN-PAGE analysis of mock-transfected cells and cells transfected with 10 nM of siRNA for 6 days. The assembly intermediates with sizes compatible with subassemblies S1 (COX1), S2 (COX1-COX4-COX5A) and S3 are indicated. (**I**) BN-PAGE analysis of HEK293T that were mock-transfected or transfected with 10 nM siRNA #2 for 6 days, and of immortalized fibroblasts from patients carrying mutations in either *SCO1* or *SURF1*. (**J**) *In vivo* mitochondrial protein synthesis. The left panel shows the incorporation of [^{35}S]methionine into mitochondrial proteins in siRNA transfected cells (10 nM, 6 days) and mock-treated cells after a 30 min pulse. The right panel highlights the stability of newly synthesized proteins 2, 3 and 4 h after washing off residual [^{35}S]methionine following the 30 min pulse.

TALENs have a high level of specificity, due in part to the 15–20 base pair length of their recognition site, we further increased the specificity of the TALENs reaction by using two TALEs fused to two endonuclease monomers that are only active upon dimerization.

Co-transfection of the TALEN pair into HEK293T cells was expected to generate double strand DNA breaks in the first exon of the *COX20* gene and, since the non-homologous end joining repair system often yields small deletions or insertions (35), an out-of frame mutation and a nonsense transcript that leads to the absence of COX20 protein. Two days after transfection, single HEK293T cells were isolated by fluorescence-activated cell sorting, amplified and screened for CIV activity immunohistochemically (not shown). Twenty of 300 clones exhibited

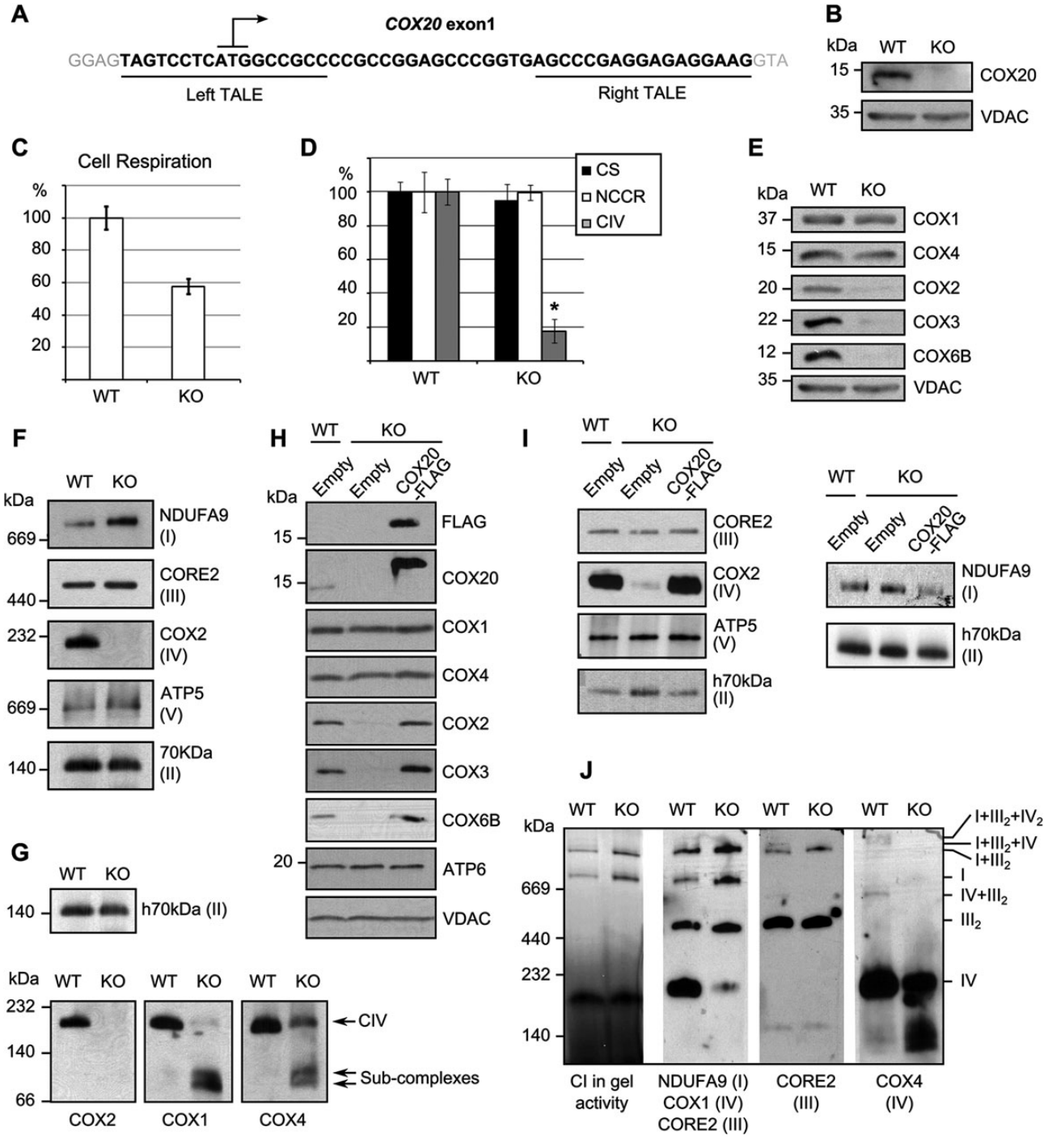

Figure 2. A KO-*COX20* cell line generated using TALENs technology exhibits an isolated CIV deficiency that is complemented by stable expression of COX20-FLAG. (**A**) Schematic representation of the first exon of the *COX20* (*FAM36A*) gene and the sequence recognition sites of both TALEs. (**B**) Immunoblot analysis of the steady-state levels of COX20 in mitochondria isolated from HEK293 T (WT) and HEK293T KO-*COX20* cell lines. VDAC was used as a loading control. (**C**) Endogenous cell respiration and (**D**) mitochondrial enzyme activities of HEK293T (WT) and HEK293T KO-*COX20* cell lines. CS, citrate synthase; NCCR, NADH-cytochrome *c* reductase (complex I + III). (**E**) Immunoblot analysis of the steady-state levels of CIV subunits in mitochondria isolated from HEK293T (WT) and HEK293T KO-*COX20* cell lines. (**F**) and (**I**) Steady-state levels of oxidative phosphorylation complexes were analyzed by BN-PAGE and detected by immunoblotting with the indicated antibodies. (**G**) BN-PAGE and immunoblot analysis of CIV subcomplexes, highlighting the accumulation of early assembly intermediates. An antibody against the h70 kDa complex II subunit was used as a loading control. (**H**) Immunoblot analysis of the steady-state levels of CIV subunits in KO-*COX20* cells alone and stably expressing COX20-FLAG compared with the parental line (WT). (**J**) Analysis of respiratory chain supercomplexes in HEK293T (WT) and the KO-*COX20* cell line, extracted with digitonin and separated by BN-PAGE. The left most panel shows an in-gel CI activity staining. The remaining three panels show immunoblots probed with the indicated antibodies.

reduced COX staining, and were selected for secondary screening. Although our COX20 antibody is suitable for immunoblotting of mitochondrial fractions, it yields an extremely poor signal in whole cell extracts. We therefore screened the steady-state levels of COX2 in these 20 clones, since its abundance is markedly decreased in *COX20* siRNA-silenced cells. Mitochondria were subsequently isolated from one of the clones with the lowest steady-state levels of COX2, and the COX20 protein was found to be undetectable by immunoblotting (Fig. 2B). Sequencing of the *COX20* gene in this clone revealed that both alleles contained mutations within the TALEN-targeted region, with a complete recombination on one allele and three point mutations on the second allele (C6A, G7T and C10G) that resulted in two amino acid changes (Ala3Ser, Pro4Ala). We presume that these point mutations affect the import or stability of the protein, since COX20 is undetectable in this clone (Fig. 2B), henceforth referred to as KO-*COX20*.

The KO-*COX20* cell line shows a profound decrease in CIV levels and activity

Knockout of *COX20* in HEK293T cells reduced the respiratory capacity to ~50% of the parental line (Fig. 2C), an effect that was a direct consequence of a severe, isolated CIV deficiency (Fig. 2D). Consistent with these observations, and like *COX20* siRNA-silenced cells (Fig. 1), the steady-state levels of COX2 and COX3 were markedly decreased in KO-*COX20* mitochondria, while those of COX1 and COX4 were unchanged (Fig. 2E). The abundance of COX6B, which is readily detected in isolated mitochondria, was also significantly reduced (Fig. 2E). BN-PAGE analysis using CII as a loading control further demonstrated very low residual levels of fully assembled CIV in the KO-*COX20* cell line, whereas the other OXPHOS complexes were unaffected (Fig. 2F). We additionally observed a marked accumulation of the CIV S1 and S2 assembly intermediates that contain COX1 and COX4 (Fig. 2G), again reflecting a block in the incorporation of COX2 into the S2 assembly intermediate (27,36,37).

The CIV assembly defect we observed in the KO-*COX20* cell line was fully restored by stable expression of C-terminal, FLAG-tagged COX20 (Fig. 2H and I), eliminating the possibility that our results were attributable to off-target effects that arose during the gene disruption procedure. Next, we investigated the effect of knocking out COX20 on the ability of respiratory complexes to form supercomplexes, by analyzing digitonized whole cell extracts using BN-PAGE. The KO-*COX20* cell line showed normal levels of I-III_2 complexes but supercomplexes containing CIV ($III_2 + IV$ and $I + III_2 + IV_n$) were too scarce to be detected (Fig. 2J). In summary, our molecular and biochemical analyses of the KO-*COX20* cell line support a model whereby COX20 functions to promote the assembly of CIV but not of other respiratory chain enzyme complexes. Our results also indicate that COX20 is not essential for CIV biogenesis but that it dramatically enhances the efficiency of the process.

Human and yeast COX20 are orthologs but do not function in the heterologous system

To gain further insight into the role of human COX20, we tested the reciprocal heterologous complementation of *S. cerevisiae* and human COX20. A knockout strain or cell line from each species was transfected with either *Sc*Cox20 or *Hs*COX20. The yeast *Sc*Cox20 is a Cox2 chaperone, whose absence leads to lack of Cox2 proteolytic cleavage by IMP and rapid Cox2 degradation. The sequence conservation between *Sc*COX20 and *Hs*COX20 is low but two hydrophobic regions are particularly conserved (Fig. 3A). Similar to *Sc*Cox20, *Hs*COX20 is an integral inner membrane protein that likely contains two transmembrane domains, with its C- and N-termini localized to the intermembrane space [(23) and Supplementary Material, Fig. S1]. Notably, *Sc*Cox20 has a 58 amino acid N-terminal extension that is missing in *Hs*COX20.

We expressed *Hs*COX20-HA, *Sc*NΔ58Cox20-HA and *Sc*Cox20-HA from either episomal or integrative vectors in a Δ*cox20* yeast strain. *Sc*Cox20-HA complemented the respiratory defect of Δ*cox20* yeast, but the human protein did not (Fig. 3B), even though it was expressed and imported into mitochondria (Fig. 3C). Although the truncated NΔ58 version of *Sc*Cox20 was also unexpectedly imported into mitochondria (Fig. 3C), and markedly complemented the growth defect of Δ*cox20* yeast on respiratory media, the Cox2 precursor was inefficiently processed in this strain (Fig. 3D) and the steady-state levels of mature Cox2 were only ~30% of wild-type. Therefore, the N-terminus of *Sc*Cox20 may be particularly important for Cox2 processing, and may in fact be involved in the interaction with the IMP peptidase, which would explain why this N-terminal region is not conserved in humans where there is no proteolytic processing of COX2.

In the reciprocal complementation studies, the CIV assembly defect in the human KO-*COX20* cell line was not rescued by stably expressing yeast Cox20 or NΔ58Cox20 (Fig. 3E and F). The lack of reciprocal complementation suggests that the sequence divergence between *Sc*Cox20 and *Hs*COX20 (Fig. 3A) prevents each protein from interacting with functional partners in the heterologous context.

Human COX20 stabilizes COX2 by interacting with the newly synthesized protein

To test the effect of *Hs*COX20 on COX2 biogenesis, we examined the synthesis and stability of newly synthesized COX2 in the KO-*COX20* cell line. Pulse-chase [^{35}S]methionine labeling showed that COX2 and all other mitochondrial proteins were synthesized at normal rates in the KO-*COX20* cell line (Fig. 4A). However, like *COX20* siRNA-silenced cells, newly synthesized COX2 and COX3 but not COX1 were unstable following a 1 h chase (Fig. 4A). Nascent ATP6 was also found to be labile, although its steady-state levels (Fig. 2H) and the abundance of the F_1F_o ATPase (Fig. 2F and I) were unaffected. The stability of newly synthesized COX2 and of other mitochondrial polypeptides in KO-*COX20* cells was restored to wild-type levels by overexpressing COX20-FLAG (Fig. 4B).

To address if *Hs*COX20 acts as a COX2 chaperone like its yeast counterpart, we next investigated whether COX20 physically interacts with COX2 or any other newly synthesized mitochondrial proteins. For this purpose, we labeled these proteins with [^{35}S]methionine in whole KO-*COX20* cells stably expressing functional COX20-FLAG, and adsorbed a mitochondrial extract onto anti-FLAG-agarose beads. We observed that of the [^{35}S]methionine-labeled proteins that were recovered from the beads, COX2 was selectively enriched when compared

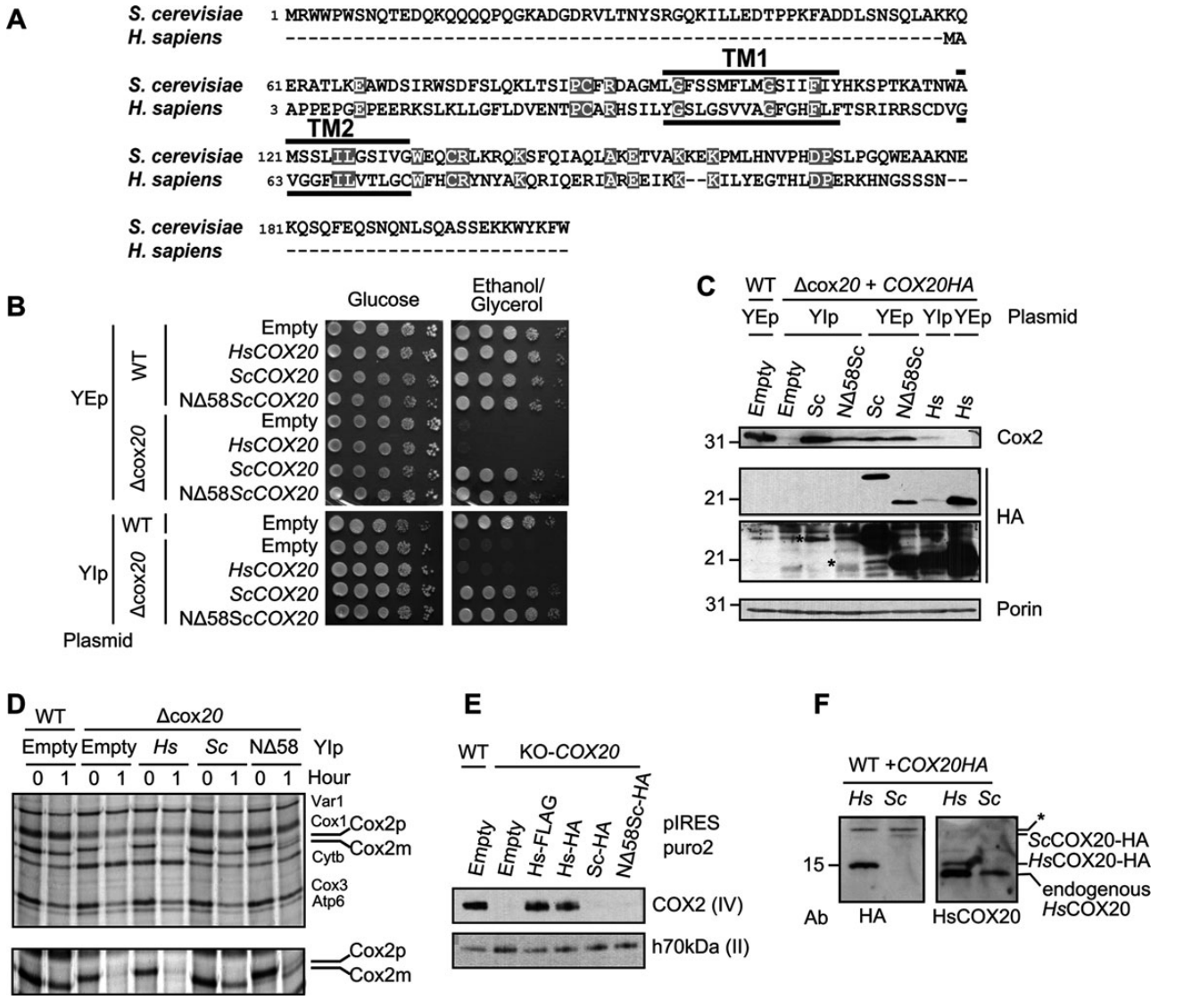

Figure 3. *Sc*Cox20 and *Hs*COX20 do not functionally substitute for each other in the heterologous systems. (**A**) Alignment of *Hs*COX20 and *Sc*Cox20. The localization of the two predicted transmembrane domains is indicated. (**B**) Serial dilutions of wild-type (WT) and Δ*cox20* W303 yeast strains on fermentable (glucose) and respiratory (ethanol + glycerol) media. *H. sapiens COX20* (*HsCOX20*), *S. cerevisiae COX20* (*ScCOX20*) and a *S. cerevisiae COX20* lacking the first 58 first amino acids (NΔ58*Sc*COX20) were expressed from either a multicopy (YEp) or an integrative (YIp) plasmid under the control of a *TEF1* promoter. (**C**) Steady-state levels of Cox20-HA and Cox2 in mitochondria isolated from the indicated yeasts strains. The two panels presented for the anti-HA reaction are two different exposure times. In the overexposed panel, the asterisks indicate faint bands of *Sc*COX20-HA and NΔ58*Sc*COX20-HA when expressed from an integrative plasmid. Porin was used as a loading control. (**D**) Radiolabeling of mitochondrial proteins synthesized during a 15-min pulse followed by a 1-hour chase. Cox2p, Cox2 precursor; Cox2 m, Cox2 mature. (**E**) BN-PAGE of HEK293T KO-*COX20* cell lines stably expressing *Hs*COX20-FLAG, *Hs*COX20-HA, *Sc*Cox20-HA or NΔ58*Sc*Cox20-HA. (**F**) Immunoblot analysis of COX20 protein levels in mitochondria purified from HEK293T (WT) stably expressing *Hs*COX20-HA or *Sc*Cox20-HA. The asterisk represent a non-specific band that crossreacts with the HA antibody.

with the parental line (Fig. 4C). COX20-FLAG was even able to co-immunoprecipitate (IP) a small fraction of the total COX2 in mitochondrial extracts from unlabeled cells (Fig. 4D). Taken together, these observations argue that the stabilizing effect of COX20 on CIV subunits is due to a direct interaction of COX20 with newly synthesized COX2.

Human COX20 is part of a ∼90 kDa complex whose stability is independent of mitochondrial protein synthesis

To better understand the function of COX20 in COX2 maturation, we analyzed its native molecular mass. BN-PAGE analysis of KO-*COX20* + COX20-FLAG whole cell extracts using an anti-FLAG antibody detected a complex of ∼90 kDa (Fig. 5A). A comparable result was obtained by analyzing the sedimentation properties in sucrose gradients of COX20 extracted from KO-*COX20* + COX20-FLAG mitochondria under the same conditions used for the immunoprecipitation experiments (Fig. 5B). These results indicate that the ∼15 kDa COX20 protein forms a stable ∼90 kDa complex in mitochondria by interacting with unidentified partners or by forming a homohexamer.

According to proteomics studies [see Protein Abundance Across Organisms (http://pax-db.org)], the molar amount of

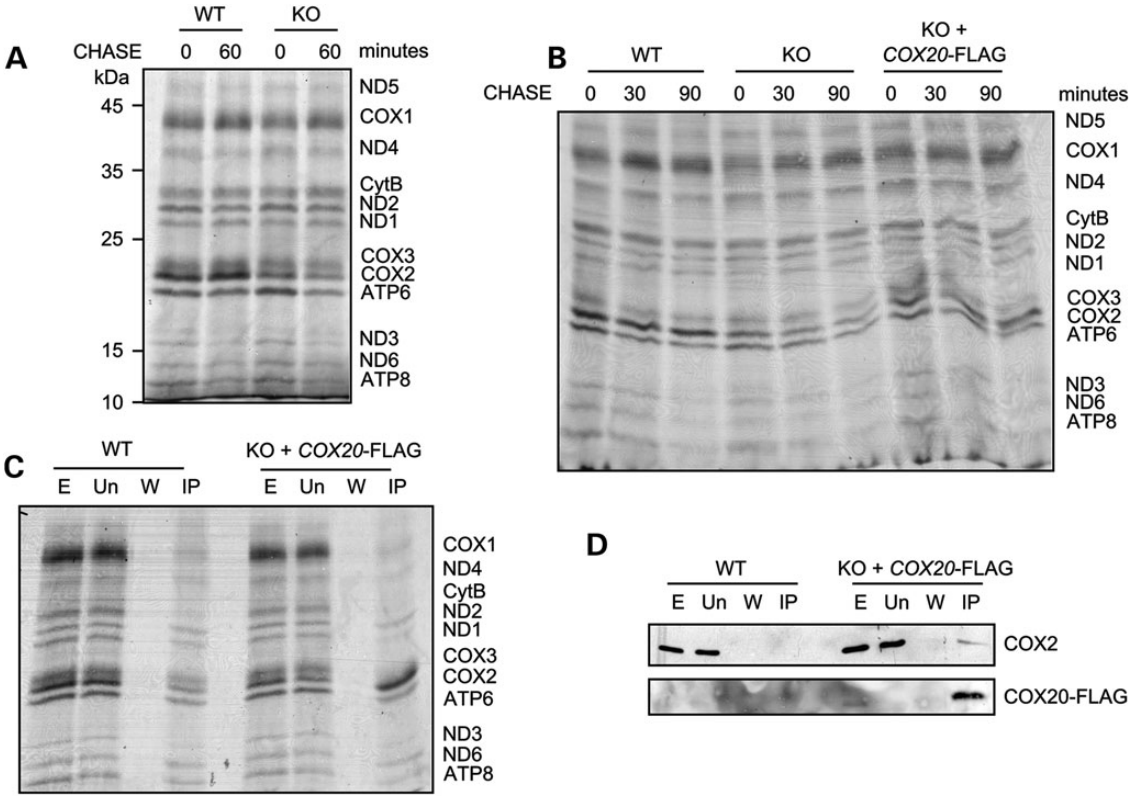

Figure 4. COX20 interacts with and stabilizes newly synthesized COX2. (**A**) and (**B**) Mitochondrial translation products were pulse-labeled with [^{35}S]methionine for 30 min in HEK293T (WT), KO-*COX20* and KO-*COX20* + COX20-FLAG cells in the presence of emetine to inhibit cytoplasmic protein synthesis, followed by the indicated chase time. Cellular protein extracts were run on an SDS–PAGE gel, transferred to nitrocellulose and exposed to film. (**C**) Mitochondrial translation products were pulse-labeled in HEK293T (WT) and KO-*COX20* + COX20-FLAG cells for 30 min. Whole cell extracts were then used for COX20-FLAG immunoprecipitation with anti-FLAG-conjugated agarose beads. E, Extract; Un, Unbound; W, Wash and IP, immunoprecipitate. (**D**) Immunoprecipitation of COX20-FLAG from mitochondrial extracts prepared from a KO-*COX20* + COX20-FLAG stable cell line using FLAG-conjugated agarose beads. Resultant membranes were immunoblotted with COX2 and FLAG antibodies. HEK293T (WT) mitochondrial extracts were used as a negative control.

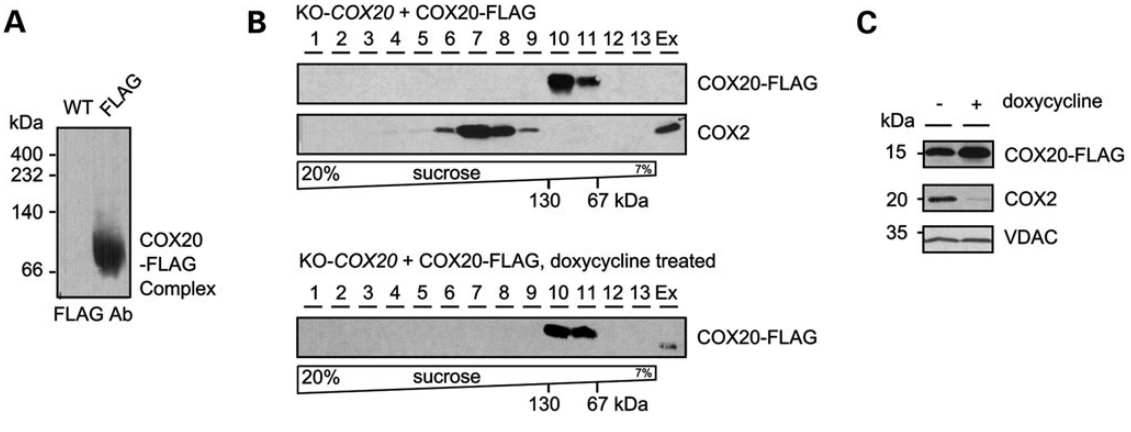

Figure 5. COX20 forms a stable complex of ~ 90 kDa independent of COX2 synthesis. (**A**) BN-PAGE of whole cell extracts from HEK293 T (WT) and KO-*COX20* + COX20-FLAG cell lines, with the resultant immunoblot decorated with FLAG antibody. (**B**) Sucrose gradient analyses of KO-*COX20* + COX20-FLAG mitochondrial extracts prepared from cells grown overnight in the absence (upper panel) or presence of 15 μg/ml of doxycycline to inhibit mitochondrial protein synthesis. The gradient was calibrated with hemoglobin (67 kDa) and lactate dehydrogenase (130 kDa). Ex, Extract. (**C**) Steady-state levels of proteins in mitochondria isolated from untreated and doxycycline-treated cells.

COX20 is 10–20 fold lower than the amount of CIV subunits, including COX2 (Supplementary Material, Table S1). Although COX20 is a low abundance protein and the COX20–COX2 interaction, we described earlier is expected to be transient in nature, the possibility nonetheless existed that the ~90 kDa COX20-containing complex includes newly synthesized COX2 or represents a COX2-containing CIV assembly intermediate. However, sucrose gradient analyses failed to detect co-sedimentation of

COX20-FLAG and COX2 (Fig. 5B), which accumulated in fractions containing the CIV monomer. Because the sucrose gradient analysis is less sensitive than the co-immunoprecipitation assays, where eluates were concentrated several fold (Fig. 4D), we further explored the relevance of COX2 to the native size of COX20 by investigating whether the integrity of the ~90 kDa complex depends on the presence of newly synthesized COX2. For this purpose, KO-*COX20* + COX20-FLAG cells were treated overnight with doxycycline to inhibit organelle protein synthesis and hence deplete the cells of newly synthesized mitochondrial polypeptides, including COX2 (Fig. 5C). Doxycycline treatment did not affect the stability of COX20-FLAG (Fig. 5C), which still sedimented in sucrose gradients as a ~90 kDa complex (Fig. 5B). These results indicate that the majority of COX20 exists in a ~90 kDa complex whose stability is independent of COX2.

COX20 interacts with SCO1 and SCO2 in a COX2-dependent manner

To gain further insight into how the chaperone function of COX20 assists with COX2 stability, we sought to assess whether other known CIV assembly factors critical to the maturation of COX2 transiently interact with COX20. For this purpose, we took a candidate approach, and concentrated on OXA1L, COX18, SCO1 and SCO2. Yeast Oxa1 is required for co-translational translocation and insertion of Cox2 into the inner membrane (38–40), and human OXA1L can functionally substitute for yeast Oxa1 (41). Human COX18 is the uncharacterized putative ortholog of *S. cerevisiae* Cox18, which is necessary for the export of the C-terminal domain of yeast Cox2 (42). Human *SCO1* and *SCO2* code for essential metallochaperones with cooperative functions in the biosynthesis of the Cu_A site in COX2 (27). SCO2 is required for efficient COX2 synthesis, and also acts as a thiol-disulfide oxidoreductase to oxidize the copper-coordinating cysteines in SCO1 during COX2 maturation (43). While COX18 could not be included in our co-immunoprecipitation experiments due to the poor quality of the commercially available antibody, OXA1 was not specifically pulled down with COX20-FLAG (Fig. 6A). In contrast, a small portion of both SCO1 and SCO2 was specifically and reproducibly co-IP with COX20-FLAG (Fig. 6A and D). The interaction between COX20 and SCO1 was subsequently confirmed by reciprocal immunoprecipitation with a SCO1 antibody (Fig. 6B). To evaluate whether the interaction between COX20 and SCO, proteins was direct or whether it was mediated through COX2, the immunoprecipitation experiment was repeated using cells that had been pretreated overnight with doxycycline to inhibit mitochondrial protein synthesis. The steady-state levels of COX2 were markedly decreased in doxycycline-treated cells, whereas the abundance of COX20 and, to a lesser extent, of SCO1 and SCO2 remained more stable (Fig. 6C). Importantly, SCO1 and SCO2 were no longer co-IP with COX20-FLAG (Fig. 6D), indicating that these interactions depend on the presence of COX2. Finally, the sedimentation of SCO1 and SCO2 in a sucrose gradient is not affected by the absence of COX20 (Fig. 6E), supporting the transient nature of their interaction and suggesting that only a small fraction of the total SCO1 or SCO2 protein pool interacts with COX20. Consistent with this idea, although siRNA knockdown of COX20 did not affect COX2 abundance in control fibroblasts, it reduced the steady-state levels of COX2 in *SCO* patient fibroblasts (Fig. 6F), which exhibit very low levels of residual SCO1 or SCO2 protein function. These results strongly suggest that COX20 binds to newly synthesized COX2 to stabilize the protein and present it to SCO1 and SCO2 to promote the maturation of its Cu_A site.

DISCUSSION

This study presents several lines of evidence demonstrating that human COX20 functions as a CIV assembly factor by stabilizing newly synthesized COX2 and promoting the maturation of its Cu_A site. First, silencing of *COX20* expression by RNAi or gene knockout (KO-*COX20*) in HEK293T cells resulted in a severe, isolated CIV deficiency that was caused by marked instability of newly synthesized COX2. Overexpression of FLAG-tagged COX20 eliminated the accumulation of early assembly intermediates in KO-*COX20* cells and rescued the CIV deficiency, confirming that the observed phenotypes were indeed a direct consequence of manipulating *COX20* expression. Second, COX20 interacts with and stabilizes newly synthesized COX2, presumably by facilitating its co-translational insertion into the mitochondrial inner membrane. Third, COX20 also physically interacts with the copper metallochaperones SCO1 and SCO2, which are known to fulfill independent but cooperative roles in the biosynthesis of the Cu_A site of COX2. Finally, siRNA knockdown of COX20 reduces the abundance of COX2 in fibroblasts derived from *SCO1* and *SCO2* patients, but not from controls, providing functional genetic evidence that further supports the importance of the physical interactions between these three proteins to the maturation of COX2.

Our current understanding of COX2 synthesis and its subsequent maturation stems from functional studies of yeast mutants and cell lines derived from patients, all of which exhibit an isolated CIV deficiency. In yeast, nascent pCox2 interacts with the Oxa1 machinery, which facilitates the insertion of the first transmembrane domain and concomitant export of the soluble N-terminal domain of pCox2 across the inner membrane (38,44). *Sc*Cox20 most likely interacts with pCox2 after export of its N-terminus (16), and facilitates both the proteolytic removal of the N-terminal presequence and the export of the C-terminal tail of pCox2 (20,45,46). Consistent with the existing yeast data (16), our immunoprecipitation results indicate that human COX20 does not physically interact with OXA1L. Although Cox18 acts on pCox2 after the cleavage of its leader sequence (47), and a Cox2-dependent interaction between Cox20 and Cox18 was recently reported in yeast (16), we were unable to address the potential conservation of this interaction in the human system because of the unavailability of high-quality COX18 antibodies.

It has been proposed that yeast Cox20 remains bound to mature Cox2 once the leader sequence of Cox2 has been cleaved, stabilizing the protein and facilitating its eventual incorporation into early CIV assembly intermediates (20). Our results demonstrate that although the yeast and human proteins are not functional in the heterologous system, human COX20 fulfills an evolutionarily conserved function by interacting with newly synthesized COX2 to promote its stability. We also show that COX20 physically

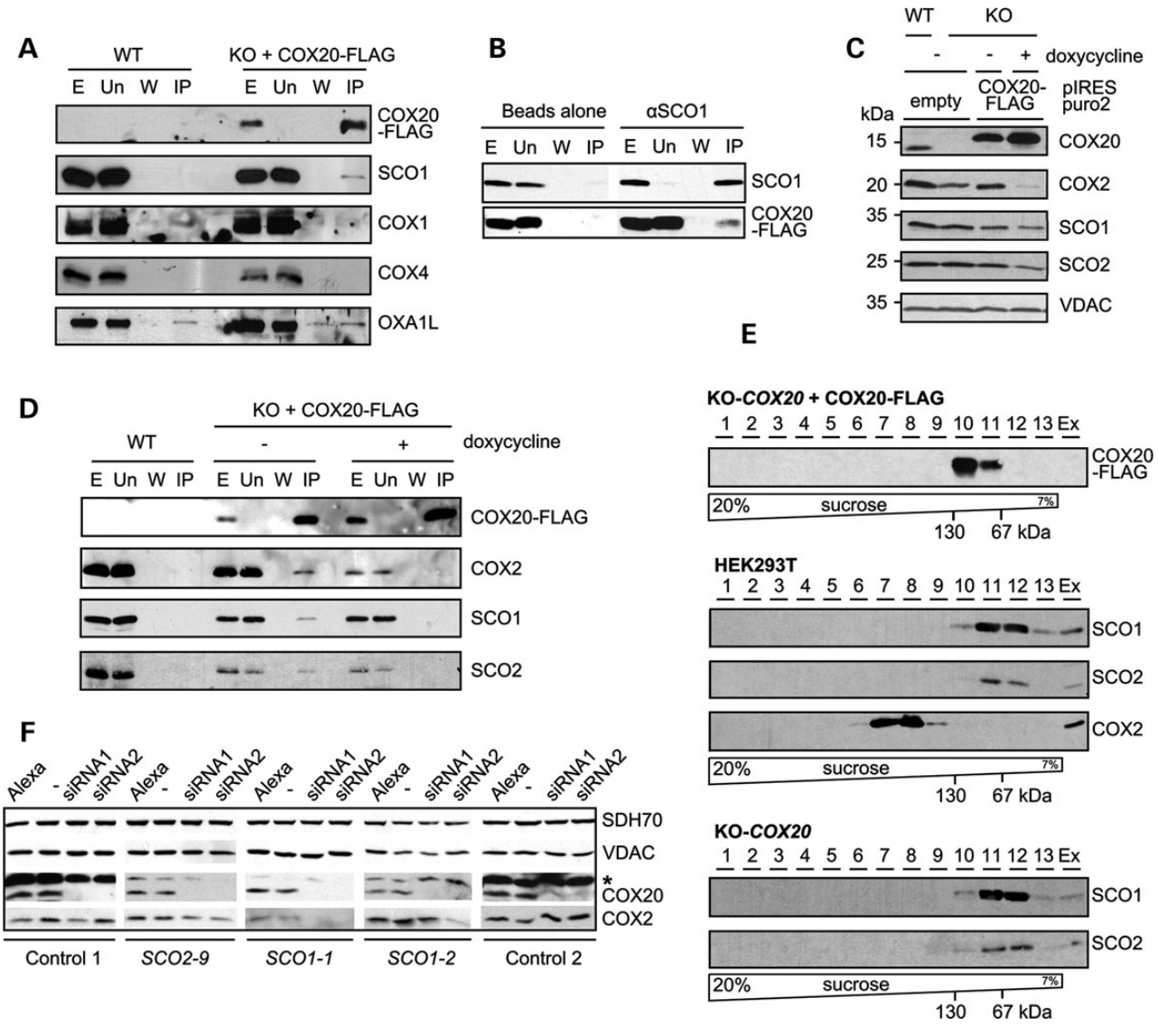

Figure 6. Transient interactions between COX20 and SCO1 and SCO2 depend on COX2 and are required for maturation of the newly synthesized polypeptide. (**A**) Immunoprecipitation of COX20-FLAG from mitochondria. E, Extract; Un, Unbound; W, Wash and IP, immunoprecipitate. The resultant blot was probed with FLAG, SCO1 and OXA1L antibodies. (**B**) Immunoprecipitation of SCO1 from KO-*COX20* + COX20-FLAG mitochondria. An anti-SCO1 antibody was conjugated with protein A Dynabeads (Invitrogen) and incubated with mitochondrial extracts. The blot was probed with SCO1 and FLAG antibodies. (**C**) Steady-state levels of COX20, COX2, SCO1 and SCO2 in purified mitochondria isolated from cells grown overnight in the absence or presence of 15 μg/ml of doxycycline. (**D**) Immunoprecipitation of COX20-FLAG using FLAG antibody-conjugated beads from mitochondrial extract of HEK293T, KO-*COX20* and KO-*COX20* + COX20-FLAG cells grown overnight in the absence or presence of doxycycline. (**E**) Sucrose gradient analyses of KO-*COX20* + COX20-FLAG, HEK293 T and KO-*COX20* mitochondrial extracts. The gradient was calibrated with hemoglobin (67 kDa) and lactate dehydrogenase (130 kDa). Ex, Extract. **(F)** Control, *SCO1* (*SCO1-1*, *SCO1-2*) and *SCO2* patient fibroblasts were grown for 9 days in basal media (−) or transfected on Days 0, 3 and 6 with one of two COX20 siRNAs (siRNA1 and siRNA2) or a scrambled siRNA (Alexa). Digitonized mitoplasts were prepared from these fibroblasts, extracted in PBS containing 1.5% lauryl maltoside and a complete protease inhibitor cocktail and equal amounts of protein (15 μg/lane) were separated by SDS–PAGE and blotted with the indicated antibodies. The asterisk indicates a non-specific band that crossreacts with the COX20 antibody.

interacts with the COX2 metallochaperones SCO1 and SCO2 in a COX2-dependent manner, strongly suggesting that the Cu_A site of human COX2 is matured while it is bound to COX20. This contention is indirectly supported by the fact that KO-*COX20* cells and fibroblasts from *COX20*, *SCO1* and *SCO2* patients all accumulate the S2 assembly intermediate, which contains COX1-COX4-COX5A but lacks COX2. Consistent with the idea that physical interactions between COX20 and SCO1 and SCO2 are important to the maturation of the Cu_A site, the steady-state levels of COX2 were reduced upon siRNA knockdown of COX20 in *SCO1* and *SCO2* patient fibroblasts, which harbor pathogenic alleles that code for highly unstable mutants or allelic variants that have little residual function. Future studies will be required to glean mechanistic insight into the ordered protein–protein interactions that promote the stability and metallation of COX2, and will likely benefit from our efforts to identify whether the stable ∼90 kDa complex containing COX20 is a homohexamer or a hetero-oligomeric stabilization complex.

We feel it is important to emphasize that while the findings of our study and of those focused on *COX20* patients (23,30) support a role for COX20 as a COX assembly factor, human COX20 is unlike its yeast counterpart in that it is not essential for CIV assembly. While it is conceivable that the Thr52Pro mutant expressed by both *COX20* pedigrees retains sufficient residual function to adequately stabilize COX2 and promote its maturation (23), even HEK293T cells lacking COX20 retain roughly 20% of the CIV activity present in the parental line. However, because the CIV deficiency is much more severe in *COX20* patient muscle when compared with patient fibroblasts (23), an intriguing possibility is that COX20 function may be more important in cell types in which the kinetics of CIV assembly are faster because the holoenzyme has a shorter half-life. Fibroblasts may also be less sensitive to loss of COX20 function because they possess alternate, COX20-independent CIV assembly mechanisms. While cell types from a greater number of *COX20* pedigrees will need to be characterized prior to drawing any definitive conclusions about the tissue-specific requirement of COX20 function, the clinical course of disease in those *COX20* patients identified to date is undeniably mild when compared with that in patients with mutations in other COX assembly factors. In summary, we used the innovative TALENs technology to generate a *COX20* knockout cell line, which allowed us to demonstrate that human COX20 is a chaperone that stabilizes COX2 and interacts with the COX2-specific metallochaperones SCO1 and SCO2 to promote Cu_A site maturation, thereby facilitating COX2 insertion into the assembling CIV holoenzyme.

MATERIALS AND METHODS

Human cell lines, transfection and culture conditions

HEK293T, HeLa and fibroblast cell lines were cultured in DMEM containing 10% FBS, 1 mM pyruvate and 50 μg/ml uridine at 37°C under 5% CO_2. Cells were transfected with lipofectamine 2000 (Invitrogen), mixed with plasmids in OPTIMEM-I media (Gibco). Stable lines were established by transfection of HEK293 T or KO-*COX20* cell lines with pIRESpuro2 empty vector or pIRESpuro2 containing variants of *COX20*. Two days after transfection, the media was supplemented with 2.5 μg/ml puromycin and drug selection was maintained for at least 1 month. Patient cell lines included a SURF1-deficient line carrying a homozygous frameshift mutation (48), and several SCO-deficient cell lines all compound heterozygotes, carrying a nonsense mutation on one allele and one of three missense mutations on the second allele (*SCO1–1*, P174L; *SCO1-2*, M294V; *SCO2*, E140 K) (28).

siRNA transfection

Two Stealth RNAi duplexes against human *COX20* (HSS151056 siRNA1, HSS151057 siRNA2, Invitrogen) were used to knock down *COX20* expression. Cells were transfected using Lipofectamine RNAiMAX (Invitrogen) according to the manufacturer's specifications on Days 0, 3 and 6. HEK293T cells (10 nM) and fibroblasts (12.5 nM) were transiently transfected with each siRNA, a scrambled control [BLOCK-iT Alexa Fluor (Invitrogen)] or mock transfected.

Plasmids

TALEN plasmids were obtained from Cellectis (Paris, France). The left and right TALENs were designed to bind the TAGTCCTCATGGCCGCC and the GAGCCCGAGGAGAGGAA DNA sequences, respectively, at the *COX20* locus. The left TALEN expresses a TALE with the variable amino acids: NI-NN-NG-HD-HD-NG-HD-NI-NG-NN-NN-HD-HD-NN-H-D-NG and the right: NG-HD-HD-NG-HD-NG-HD-HD-NG-HD-NN-NN-NN-HD-NG-NG.

HsCOX20-1HA and *HsCOX20*-1FLAG were amplified by PCR using the *COX20* cDNA (Sequence Genbank BC0118519.1) as a template. *ScCOX20*-HA and NΔ58*ScCOX20*-HA were amplified by PCR from genomic DNA from the yeast W303 strain. All four amplicons were then cloned into pIRESpuro2 using *Nhe*I and *BamH*I sites. *HsCOX20*-1HA, *ScCOX20*-HA and NΔ58*ScCOX20*-HA were cloned as *Hind*III and *Xba*I fragments into the yeast multicopy expression plasmid YEplac112 and the integrative plasmid YIplac128 (*Xba*I and *BamH*I), under the control of the *ScTEF1* promoter. The oligonucleotides used for cloning in this study are listed in Supplementary Material, Table S2.

Antibodies

An affinity-purified rabbit polyclonal antibody against a C-terminal human COX20 peptide (RYNYAKQRIQERIAREEIKK) was generated by Open Biosystems/Thermo Scientific (Huntsville, AL, USA). A human SCO1 antibody was generated by injecting rabbits with a synthetic peptide (CASIATHMRPYRKKS) that had been conjugated to KLH via a reactive sulfhydryl group (Pierce) and emulsified in Titermax (Pierce) (27). The crude polyclonal antiserum was purified by its sequential incubation with glutathione-*S*-transferase (GST) and a GST-SCO1 antigen fusion protein, each of which had been crosslinked to AminoLink (Pierce) columns according to the manufacturer's instructions. Antibody bound to the GST-SCO1 column was eluted with acetic acid, rapidly neutralized with unbuffered Tris and then buffer exchanged and concentrated in PBS containing 50% glycerol.

The following commercial antibodies were used in this study; FLAG, VDAC, HSP70 and SCO2 were from Sigma-Aldrich; ATP6, COX1, COX2, COX3, COX4, COX6b, ATP5α, NDUFA9, CORE2 and h70 kDa were from Abcam; HA was from Covance and OXA1 for LSBio. Secondary antibodies coupled to horseradish peroxidase were obtained from Santa Cruz Biotechnology. Secondary Mouse TrueBlot ULTRA (Rockland) was used for immunoblot after immunoprecipitation to eliminate interference of the heavy and light chains of the immunoprecipitating antibody.

Mitochondrial isolation

Mitochondria from human cells were isolated from at least ten 80–100% confluent 175 cm^2 flasks as described previously (49). Briefly, the cells were resuspended in ice-cold T-K-Mg buffer (10 mM Tris–HCl, 10 mM KCl, 0.15 mM $MgCl_2$, pH 7.0) and disrupted with 10 strokes in a homogenizer (Kimble/Kontes, Vineland, NJ, USA). Using a 1 M sucrose solution, the homogenate was brought to a final concentration of 0.25 M sucrose and a postnuclear supernatant was obtained by

centrifugation of the samples twice for 3 min at 1500 g. Mitochondria were pelleted by centrifugation for 10 min at 8000 g and resuspended in 0.6 M Sorbitol 10 mM Hepes pH 7.4.

Immunoblotting

Protein concentration was measured with the folin phenol reagent (50). For immunoblotting studies, 20–60 μg of mitochondrial proteins were separated by SDS–PAGE in the Laemmli buffer system (51). After transfer, membranes with immobilized proteins were decorated with antibodies against the appropriate proteins followed by a second reaction with anti-mouse or anti-rabbit IgG conjugated to horseradish peroxidase (Sigma, St Louis, MO, USA). Chemiluminescence was used for the final detection.

Mitochondrial protein synthesis

Mitochondrial protein synthesis was determined in human cells by pulse-labeling 80% confluent cell cultures growing in a 6-well plate in media supplemented with 100 μl/ml emetine (for pulse assays) or 100 μl/ml anisomycin (for pulse-chase assays) to inhibit cytoplasmic protein synthesis as described (52). Subsequently, whole cell extracts were prepared by solubilization in RIPA buffer (1% NP-40, 0.1% SDS, 50 mM Tris–HCl pH 7.4, 150 mM NaCl, 0.5 sodium deoxycholate, 1 mM EDTA) with 1 mM PMSF and 1 × mammalian protease inhibitor cocktail (Sigma). In yeast, mitochondrial gene products were labeled with [^{35}S]-methionine (7 mCi/mmol, Perkin Elmer) in whole cells at 30°C in the presence of 0.2 mg/ml cycloheximide to inhibit cytoplasmic protein synthesis (53). Equal amounts of total cellular protein (human or yeast) were loaded in each lane and separated by SDS–PAGE on a 17.5% polyacrylamide gel, transferred to a nitrocellulose membrane and exposed to Kodak X-OMAT X-ray film.

Immunoprecipitation

For immunoprecipitation of COX20-FLAG, 600 μg of mitochondria were extracted in 400 μl of 20 mM Tris pH 7.5, 50 mM KCl, 0.4% lauryl maltoside, 1 mM PMSF and 1 × protease inhibitor cocktail. The lysate was centrifuged at 22 000*g*, 30 min at 4°C. The extract (E) was incubated for 4 h at 4°C with 30 μl beads conjugated with a FLAG antibody (anti-DYKDDDDK beads, Clontech) or SCO1 antibody conjugated to protein A beads (Invitrogen). The unbound material (Un) was removed and the beads were washed three times in 400 μl of 20 mM Tris pH 7.5 50 mM KCl buffer. The beads were then supplemented with 60 μl of Laemmli buffer to release the IP material. Representative amounts of all fractions were boiled, and loaded on an SDS–PAGE gel in the following proportions; E (1 ×), Un (1 ×), Wash (1 ×) and IP (10 ×).

For co-immunoprecipitation studies of COX20-FLAG with newly synthesized mitochondrial translation products, subconfluent cells were radiolabeled with [^{35}S]methionine for 30 min in the presence of emetine to inhibit cytoplasmic protein synthesis. Cells were then washed with PBS and trypsinized. 7.5 × 10^6 cells were incubated 10 min with 2 mg/ml of digitonin (Sigma), spun at 10 000 g for 5 min at 4°C. Digitonized cell pellets were washed with PBS, and solubilized in 380 μl of 20 mM Tris pH 7.5, 50 mM KCl, 0.4% lauryl maltoside, 1 mM PMSF and 1 × protease inhibitor cocktail. Finally, the resultant extracts were used for COX20-FLAG immunoprecipitation using 20 μl of anti-FLAG-conjugated agarose beads, as described earlier.

Determination of cellular respiration and mitochondrial enzyme activities

Potassium cyanide (KCN)-sensitive endogenous cell respiration was measured polarographically in cells from a 70% confluent flask. Growth media was changed 3 h prior to trypsinizing the cells. Cells were resuspended in DMEM + 10 mM HEPES pH 7.2 buffer, and oxygen consumption was measured using a Clark oxygen electrode in a micro water-jacketed, magnetically stirred cell set at 37°C (Hansatech Instruments Limited, Norfolk, UK). The reaction was inhibited with KCN (700 μM) to obtain the baseline rate, as described (54). All values were normalized to the total cell number.

The activities of the OXPHOS complexes [CI + CIII or NADH-cytochrome *c* reductase (NCCR) and CIV] and the TCA enzyme citrate synthase were determined spectrophotometrically in freeze-thawed cells as described previously (54). In-gel complex I activity was determined by incubating a BN-PAGE in 2 mM Tris–HCl pH 7.4, 0.1 mg/ml NADH (Sigma) with 2.5 mg/ml iodotetranitrozolium (Sigma) (55).

BN-PAGE analysis

The abundance of OXPHOS complexes was analyzed by BN-PAGE using a linear 3–12% gradient gel. 2.5 × 10^6 cells were incubated in 200 μl of PBS and 70 μl of 8 mg/ml digitonin (Sigma) at 4°C 10 min. Cells were spun at 10 000*g* for 5 min at 4°C and washed two times in PBS. Pellets were resuspended in 100 μl of 1.5 M amminocaproic acid, 50 mM Bis–Tris pH 7.0 and 1 μl of 20% lauryl maltoside (for isolated monomeric complexes analysis) or 10 μl of 10% digitonin (for supercomplexes analysis). After spinning at 22 000*g* for 30 min at 4°C, the clarified extracts were supplemented with 10 μl of 750 mM aminocaproic acid, 50 mM Bis–Tris pH 7.0, 0.5 mM EDTA and 5% serva blue G. For each sample, extracts from ∼2.5 to 5 × 10^5 cells were loaded in the gel.

Sucrose gradient analysis

The native mass of COX20 was estimated by following its sedimentation properties in linear sucrose gradients. Mitochondria (1 mg) were extracted in 300 μl of 20 mM Tris pH 7.5, 50 mM KCl, 0.4% lauryl maltoside, 1 mM PMSF and 1 × protease inhibitor cocktail. The lysate was spun at 22 000 g for 30 min at 4°C, and the clarified extract was loaded onto a 5 ml 7–20% sucrose gradient containing 20 mM Tris pH 7.5, 50 mM KCl, 0.1% lauryl maltoside and 1 mM PMSF buffer and centrifuged at 28 000 g for 14 h at 4°C. The gradients were fractionated into 13 fractions, TCA precipitated and the pellets resuspended in Laemmli buffer and analyzed by immunoblotting. For each round of ultracentrifugation, a control gradient was loaded with two calibration standards in extraction buffer; 2 mg of hemoglobin and 20 μl of bovine heart lactate dehydrogenase (1000 units/ml, Sigma).

Saccharomyces cerevisiae strains and methods

All yeast strains were in the W303 background (a *ade2-1 his3-1,15 leu2-3,112 trp1-1 ura3-1*). A W303Δ*cox20* strain was obtained from Dr A. Tzagoloff (20). The growth media compositions of yeast strains have been described elsewhere (56). Yeast mitochondrial isolation and *in vivo* protein synthesis were performed as reported (53,57). The *Sc*Cox2 and porin antibodies were obtained from Molecular Probes and Abcam, respectively.

Statistical analysis

All experiments were done at least in triplicate. All data are presented as means ± SD of absolute values or the percentage of control. Values were analyzed for statistical significance by Student's *t*-test. $P < 0.05$ was considered significant.

SUPPLEMENTARY MATERIAL

Supplementary Material is available at *HMG* online.

ACKNOWLEDGEMENTS

We thank Dr Iliana Soto for critical reading of the manuscript. We thank Dr Tzagoloff for providing reagents.

Conflict of Interest statement. None declared.

FUNDING

This research was supported by an American Heart Association (AHA) postdoctoral fellowship (to M.B.), and grants-in-aid of research from the NIH (GM071775-06, A.Ba), MDA (A.Ba) and CIHR (S.C.L.). S.C.L. is a New Investigator of the CIHR.

REFERENCES

1. Shoubridge, E.A. (2001) Cytochrome *c* oxidase deficiency. *Am. J. Med. Genet.*, **106**, 46–52.
2. Zee, J.M. and Glerum, D.M. (2006) Defects in cytochrome oxidase assembly in humans: lessons from yeast. *Biochem. Cell Biol.*, **84**, 859–869.
3. Pecina, P., Houstkova, H., Hansikova, H., Zeman, J. and Houstek, J. (2004) Genetic defects of cytochrome *c* oxidase assembly. *Physiol. Res.*, **53**, S213–S223.
4. Fontanesi, F. and Barrientos, A. (2013) In Wong, L.E. (ed.), *Mitochondrial Disorders Caused by Nuclear Genes. Part 3*. Springer Science, New York, pp. 239–259 (in press).
5. Tsukihara, T., Aoyama, H., Yamashita, E., Tomizaki, T., Yamaguchi, H., Shinzawa-Itoh, K., Nakashima, R., Yaono, R. and Yoshikawa, S. (1996) The whole structure of the 13-subunit oxidized cytochrome c oxidase at 2.8 A. *Science*, **272**, 1136–1144.
6. Ostermeier, C., Harrenga, A., Ermler, U. and Michel, H. (1997) Structure at 2.7 A resolution of the *Paracoccus denitrificans* two-subunit cytochrome c oxidase complexed with an antibody FV fragment. *Proc. Natl Acad. Sci. USA*, **94**, 10547–10553.
7. Yoshikawa, S., Shinzawa-Itoh, K., Nakashima, R., Yaono, R., Yamashita, E., Inoue, N., Yao, M., Fei, M.J., Libeu, C.P., Mizushima, T. *et al.* (1998) Redox-coupled crystal structural changes in bovine heart cytochrome *c* oxidase. *Science*, **280**, 1723–1729.
8. Fontanesi, F., Soto, I.C., Horn, D. and Barrientos, A. (2006) Assembly of mitochondrial cytochrome *c* oxidase, a complicated and highly regulated cellular process. *Am. J. Physiol. Cell Physiol.*, **291**, C1129–C1147.
9. Cobine, P.A., Pierrel, F. and Winge, D.R. (2006) Copper trafficking to the mitochondrion and assembly of copper metalloenzymes. *Biochim. Biophys. Acta*, **1763**, 759–772.
10. Soto, I.C., Fontanesi, F., Liu, J. and Barrientos, A. (2012) Biogenesis and assembly of eukaryotic cytochrome c oxidase catalytic core. *Biochim. Biophys. Acta*, **1817**, 883–897.
11. Bourens, M., Fontanesi, F., Soto, I.C., Liu, J. and Barrientos, A. (2013) Redox and reactive oxygen species regulation of mitochondrial cytochrome *c* oxidase biogenesis. *Antioxid. Redox Signal.*, **19**, 1940–1952.
12. Saraste, M. (1990) Structural features of cytochrome oxidase. *Q. Rev. Biophys.*, **23**, 331–366.
13. Mitchell, P. and Moyle, J. (1967) Chemiosmotic hypothesis of oxidative phosphorylation. *Nature*, **213**, 137–139.
14. Nijtmans, L.G., Taanman, J.W., Muijsers, A.O., Speijer, D. and Van den Bogert, C. (1998) Assembly of cytochrome-*c* oxidase in cultured human cells. *Eur. J. Biochem.*, **254**, 389–394.
15. McStay, G.P., Su, C.H. and Tzagoloff, A. (2013) Modular assembly of yeast cytochrome oxidase. *Mol. Biol. Cell*, **24**, 440–452.
16. Elliott, L.E., Saracco, S.A. and Fox, T.D. (2012) Multiple roles of the Cox20 chaperone in assembly of *Saccharomyces cerevisiae* cytochrome c oxidase. *Genetics*, **190**, 559–567.
17. Khalimonchuk, O., Bestwick, M., Meunier, B., Watts, T.C. and Winge, D.R. (2010) Formation of the redox cofactor centers during Cox1 maturation in yeast cytochrome oxidase. *Mol. Cell Biol.*, **30**, 1004–1017.
18. Tzagoloff, A. and Dieckmann, C.L. (1990) PET genes of *Saccharomyces cerevisiae*. *Microbiol. Rev.*, **54**, 211–225.
19. McEwen, J.E., Ko, C., Kloeckner-Gruissem, B. and Poyton, R.O. (1986) Nuclear functions required for cytochrome c oxidase biogenesis in *Saccharomyces cerevisiae*. Characterization of mutants in 34 complementation groups. *J. Biol. Chem.*, **261**, 11872–11879.
20. Hell, K., Tzagoloff, A., Neupert, W. and Stuart, R.A. (2000) Identification of Cox20p, a novel protein involved in the maturation and assembly of cytochrome oxidase subunit 2. *J. Biol. Chem.*, **275**, 4571–4578.
21. Glerum, D.M., Shtanko, A. and Tzagoloff, A. (1996) SCO1 *and* SCO2 *act as High Copy Suppressors of A Mitochondrial Copper Recruitment Defect in* Saccharomyces cerevisiae. J. Biol. Chem., 271, 20531–20535.
22. Weraarpachai, W., Antonicka, H., Sasarman, F., Seeger, J., Schrank, B., Kolesar, J.E., Lochmuller, H., Chevrette, M., Kaufman, B.A., Horvath, R. *et al.* (2009) Mutation in TACO1, encoding a translational activator of COX I, results in cytochrome *c* oxidase deficiency and late-onset Leigh syndrome. *Nat. Genet.*, **41**, 833–837.
23. Szklarczyk, R., Wanschers, B.F., Nijtmans, L.G., Rodenburg, R.J., Zschocke, J., Dikow, N., van den Brand, M.A., Hendriks-Franssen, M.G., Gilissen, C., Veltman, J.A. *et al.* (2013) A mutation in the FAM36A gene, the human ortholog of COX20, impairs cytochrome *c* oxidase assembly and is associated with ataxia and muscle hypotonia. *Hum. Mol. Genet.*, **22**, 656–667.
24. Leary, S.C., Cobine, P.A., Kaufman, B.A., Guercin, G.H., Mattman, A., Palaty, J., Lockitch, G., Winge, D.R., Rustin, P., Horvath, R. *et al.* (2007) The human cytochrome c oxidase assembly factors *SCO1* and *SCO2* have regulatory roles in the maintenance of cellular copper homeostasis. *Cell Metab.*, **5**, 9–20.
25. Zhu, Z., Yao, J., Johns, T., Fu, K., De Bie, I., Macmillan, C., Cuthbert, A.P., Newbold, R.F., Wang, J., Chevrette, M. *et al.* (1998) *SURF1*, encoding a factor involved in the biogenesis of cytochrome c oxidase, is mutated in Leigh syndrome. *Nat. Genet.*, **20**, 337–343.
26. Tiranti, V., Galimberti, C., Nijtmans, L., Bovolenta, S., Perini, M.P. and Zeviani, M. (1999) Characterization of *SURF-1* expression and Surf-1p function in normal and disease conditions. *Hum. Mol. Genet.*, **8**, 2533–2540.
27. Leary, S.C., Kaufman, B.A., Pellecchia, G., Guercin, G.H., Mattman, A., Jaksch, M. and Shoubridge, E.A. (2004) Human SCO1 and SCO2 have independent, cooperative functions in copper delivery to cytochrome *c* oxidase. *Hum. Mol. Genet.*, **13**, 1839–1848.
28. Valnot, I., Osmond, S., Gigarel, N., Mehaye, B., Amiel, J., Cormier-Daire, V., Munnich, A., Bonnefont, J.P., Rustin, P. and Rotig, A. (2000) Mutations of the *SCO1* gene in mitochondrial cytochrome c oxidase deficiency with neonatal-onset hepatic failure and encephalopathy. *Am. J. Hum. Genet.*, **67**, 1104–1109.
29. Papadopoulou, L.C., Sue, C.M., Davidson, M.M., Tanji, K., Nishino, I., Sadlock, J.E., Krishna, S., Walker, W., Selby, J., Glerum, D.M. *et al.* (1999) Fatal infantile cardioencephalomyopathy with COX deficiency and mutations in *SCO2*, a COX assembly gene. *Nat. Genet.*, **23**, 333–337.

30. Doss, S., Lohmann, K., Seibler, P., Arns, B., Klopstock, T., Zuhlke, C., Freimann, K., Winkler, S., Lohnau, T., Drungowski, M. *et al.* (2013) Recessive dystonia-ataxia syndrome in a Turkish family caused by a COX20 (FAM36A) mutation. *J. Neurol*., doi: 10.1007/s00415-013-7177-7.
31. Herrmann, J.M. and Funes, S. (2005) Biogenesis of cytochrome oxidase-sophisticated assembly lines in the mitochondrial inner membrane. *Gene*, **354**, 43–52.
32. Christian, M., Cermak, T., Doyle, E.L., Schmidt, C., Zhang, F., Hummel, A., Bogdanove, A.J. and Voytas, D.F. (2010) Targeting DNA double-strand breaks with TAL effector nucleases. *Genetics*, **186**, 757–761.
33. Miller, J.C., Tan, S., Qiao, G., Barlow, K.A., Wang, J., Xia, D.F., Meng, X., Paschon, D.E., Leung, E., Hinkley, S.J. *et al.* (2011) A TALE nuclease architecture for efficient genome editing. *Nat. Biotechnol.*, **29**, 143–148.
34. Li, T., Huang, S., Zhao, X., Wright, D.A., Carpenter, S., Spalding, M.H., Weeks, D.P. and Yang, B. (2011) Modularly assembled designer TAL effector nucleases for targeted gene knockout and gene replacement in eukaryotes. *Nucleic Acids Res.*, **39**, 6315–6325.
35. Weterings, E. and Chen, D.J. (2008) The endless tale of non-homologous end-joining. *Cell Res.*, **18**, 114–124.
36. Stiburek, L., Vesela, K., Hansikova, H., Pecina, P., Tesarova, M., Cerna, L., Houstek, J. and Zeman, J. (2005) Tissue-specific cytochrome c oxidase assembly defects due to mutations in *SCO2* and *SURF1*. *Biochem. J.*, **392**, 625–632.
37. Williams, S.L., Valnot, I., Rustin, P. and Taanman, J.W. (2004) Cytochrome *c* oxidase subassemblies in fibroblast cultures from patients carrying mutations in *COX10*, *SCO1*, or *SURF1*. *J. Biol. Chem.*, **279**, 7462–7469.
38. He, S. and Fox, T.D. (1997) Membrane translocation of mitochondrially coded Cox2p: distinct requirements for export of N and C termini and dependence on the conserved protein Oxa1p. *Mol. Biol Cell*, **8**, 1449–1460.
39. Szyrach, G., Ott, M., Bonnefoy, N., Neupert, W. and Herrmann, J.M. (2003) Ribosome binding to the Oxa1 complex facilitates co-translational protein insertion in mitochondria. *EMBO J.*, **22**, 6448–6457.
40. Jia, L., Dienhart, M., Schramp, M., McCauley, M., Hell, K. and Stuart, R.A. (2003) Yeast Oxa1 interacts with mitochondrial ribosomes: the importance of the C-terminal region of Oxa1. *EMBO J.*, **22**, 6438–6447.
41. Bonnefoy, N., Kermorgant, M., Groudinsky, O., Minet, M., Slonimski, P.P. and Dujardin, G. (1994) Cloning of a human gene involved in cytochrome oxidase assembly by functional complementation of an oxa1- mutation in *Saccharomyces cerevisiae*. *Proc. Natl Acad. Sci. USA*, **91**, 11978–11982.
42. Saracco, S.A. and Fox, T.D. (2002) Cox18p is required for export of the mitochondrially encoded *Saccharomyces cerevisiae* Cox2p C-tail and interacts with Pnt1p and Mss2p in the inner membrane. *Mol. Biol. Cell*, **13**, 1122–1131.
43. Leary, S.C., Sasarman, F., Nishimura, T. and Shoubridge, E.A. (2009) Human SCO2 is required for the synthesis of CO II and as a thiol-disulphide oxidoreductase for SCO1. *Hum. Mol. Genet.*, **18**, 2230–2240.
44. Hell, K., Herrmann, J.M., Pratje, E., Neupert, W. and Stuart, R.A. (1998) Oxa1p, an essential component of the N-tail protein export machinery in mitochondria. *Proc. Natl Acad. Sci. USA*, **95**, 2250–2255.
45. Hell, K., Herrmann, J., Pratje, E., Neupert, W. and Stuart, R.A. (1997) Oxa1p mediates the export of the N- and C-termini of pCoxII from the mitochondrial matrix to the intermembrane space. *FEBS Lett.*, **418**, 367–370.
46. Nunnari, J., Fox, T.D. and Walter, P. (1993) A mitochondrial protease with two catalytic subunits of nonoverlapping specificities. *Science*, **262**, 1997–2004.
47. Carlson, C.G., Barrientos, A., Tzagoloff, A. and Glerum, D.M. (2003) COX16 Encodes A Novel Protein Required for the Assembly of Cytochrome Oxidase in Saccharomyces Cerevisiae. *J. Biol. Chem.*, 278, 3770–3775.
48. von Kleist-Retzow, J.C., Vial, E., Chantrel-Groussard, K., Rotig, A., Munnich, A., Rustin, P. and Taanman, J.W. (1999) Biochemical, genetic and immunoblot analyses of 17 patients with an isolated cytochrome *c* oxidase deficiency. *Biochim. Biophys. Acta*, **1455**, 35–44.
49. Enriquez, J.A. and Attardi, G. (1996) Analysis of aminoacylation of human mitochondrial tRNAs. *Methods Enzymol.*, **264**, 183–196.
50. Lowry, O.H., Rosebrough, N.J., Farr, A.L. and Randall, R.J. (1951) Protein measurement with the Folin phenol reagent. *J. Biol. Chem.*, **193**, 265–275.
51. Laemmli, U.K. (1970) Cleavage of structural proteins during the assembly of the head of bacteriophage T4. *Nature*, **227**, 680–685.
52. Leary, S.C. and Sasarman, F. (2009) Oxidative phosphorylation: synthesis of mitochondrially encoded proteins and assembly of individual structural subunits into functional holoenzyme complexes. *Methods Mol. Biol.*, **554**, 143–162.
53. Barrientos, A., Korr, D. and Tzagoloff, A. (2002) Shy1p is necessary for full expression of mitochondrial *COX1* in the yeast model of Leigh's syndrome. *EMBO J.*, **21**, 43–52.
54. Barrientos, A., Fontanesi, F. and Diaz, F. (2009) Evaluation of the mitochondrial respiratory chain and oxidative phosphorylation system using polarography and spectrophotometric enzyme assays. *Curr. Protoc. Hum. Genet*. Chapter, Unit **19**, 4.1–4.13.
55. Bratic, A., Wredenberg, A., Gronke, S., Stewart, J.B., Mourier, A., Ruzzenente, B., Kukat, C., Wibom, R., Habermann, B., Partridge, L. *et al.* (2011) The bicoid stability factor controls polyadenylation and expression of specific mitochondrial mRNAs in *Drosophila melanogaster*. *PLoS Genet.*, **7**, e1002324.
56. Myers, A.M., Pape, L.K. and Tzagoloff, A. (1985) Mitochondrial protein synthesis is required for maintenance of intact mitochondrial genomes in *Saccharomyces cerevisiae*. *EMBO J.*, **4**, 2087–2092.
57. Gouget, K., Verde, F. and Barrientos, A. (2008) *In vivo* labeling and analysis of mitochondrial translation products in budding and in fission yeasts. *Methods Mol. Biol.*, **457**, 113–124.